

# SIMULATION OF DOUBLE LAYER IN DC DISCHARGE

P. Vrba

*Institute of Plasma Physics, Acad. Sci. CR  
Za Slovankou 3, CZ-182 21 Praha 8, Czech Republic*

Particle-in-cell Monte Carlo code has been used to simulate the DC discharge in strongly inhomogeneous cylindrical and spherical electric fields. The discharge threshold conditions has been specified and corresponding threshold voltage (threshold electric field intensity) has been determined numerically. The threshold voltage varies with the electrode geometry, the polarity of active electrodes, gas composition (H, Ar, N<sub>2</sub>) and gas pressure. In case of positively charged inner electrode, a thin boundary sheet is developed in the vicinity of the electrode, when the quasineutrality of ionized gas is violated and the electron current is closed via external RLC circuit. In the opposite case of negatively charged inner electrode, a double layer is developed inside ionized gas. The inner electric field of DL accelerates positively charged particles.

## 1. Introduction

The theoretical estimations for breakdown voltage and electric field are based on **the Townsend's script** of the electron avalanche in radially nonuniform electric fields [1,2]. In the case of cylindrical symmetry the formulae for breakdown potential and breakdown electric field were recalculated. In the case of spherical symmetry the compact formulae were not obtained and the breakdown voltage or breakdown electric field are determined solving transcendent equation.

The computer simulations complement the analytic model and give better understanding of the behaviour of the discharge parameters that are not available either from experimental measurements or theoretical calculations. The numerical codes **PDC1** and **PDS1**<sup>1</sup> were used to simulate the DC discharge in gaseous medium between a thin wire and coaxial cylinder, or between sharp tip and sphere at high voltage. This codes utilize **particle-in-cell (PIC) techniques** plus **Monte Carlo (MCC)** simulation. The basic idea of PIC simulation is to allow thousands of computer simulated super-particles to represent many more real particles in laboratory devices. The super-particles interact with the external or internal electric and magnetic field. The interactions between charged and neutral super-particles are describe by conventional Monte Carlo schemes, the time or distance between collisions for each particle is calculated using random numbers. The external circuit current interacts with the plasma current via surface charge on the electrodes. The potential within the bounded plasma is affected by the distribution and motion of space charge, the electrode surface charge and the external circuit current.

## 2. Theory

When the electric field between two electrodes is inhomogeneous, the successive development of electron avalanches has a local character [1]. **The breakdown condition** for the discharge can be written as

$$\int_{r_1}^{r_2} \alpha dr = \ln \left( \frac{1 + \gamma}{\gamma} \right), \quad (1)$$

---

<sup>1</sup> Available from Software Distribution Office, Industrial Liaison Program, EECS Dept., 479 Cory Hall, University of California, Berkeley, CA 94720.

where  $\alpha = pA \exp\left(-\frac{Bp}{E}\right)$  is the Townsend's first coefficient (the number of electrons produced per unit length in the field direction),  $\gamma$  is the second ionization coefficient (the yield of secondary electrons) and  $A, B = AV_i$  are coefficients depending on gas temperature,  $V_i$  is the first ionization potential of the atom.

In the case studied the radial electric field can be expressed as  $E = E_1\left(\frac{r_1}{r}\right)^n$ , where  $r_1$  is the radius of inner electrode and  $E_1$  is electric field intensity at the inner electrode.

For **cylindrical electrodes** ( $n = 1$ ,  $E_1 = \frac{U}{r_1 \ln(r_2/r_1)}$ ,  $U$  denotes the applied potential) the integration of the Townsend's first coefficient  $\alpha$ , (under the conditions  $l < r_1$ ,  $\Delta R \ll r_1$ ) leads to

$$U_b \approx \frac{Bp\Delta R}{\ln \frac{Ap\Delta R}{\ln(1+1/\gamma)}}. \quad (2)$$

It is obvious, the parameter  $p\Delta R$  has the same meaning as  $p.d$  in planar geometry [2]. This approximation is very helpful for the code verification.

For the **spherical case** ( $n = 2$ ,  $E_1 = \frac{r_2}{r_1} \frac{U}{(r_1-r_2)}$ ), the integration of the Townsend's first coefficient  $\alpha$  under the condition  $|E_1 r_1^2 / V_i r| > 1$  leads to transcendental equation

$$\frac{\sqrt{\pi}Ap}{2q} \{ \Phi[(1+\delta)qr_1] - \Phi[qr_1] \} = \ln(1+1/\gamma), \quad (3)$$

where quantity  $q = \sqrt{\frac{\delta}{1+\delta}} \sqrt{\frac{Bp}{r_1 U_b}}$  and  $\Phi(qr) = 2q/\sqrt{\pi} \int_0^r e^{-(qr)^2} dr$ . The intersection point of the functions  $f(1) = \Phi[(1+\delta)qr_1]$  and  $f(2) = \Phi[qr_1] + \frac{2q \ln(1+1/\gamma)}{\sqrt{\pi p A}}$  (see Fig. 1) determines the value of breakdown voltage  $U_b$ .

$\gamma$	material of electrode	$U_b$ Volt
0.00035	Hg	650.0
0.001	Fe	495.5
0.005	Ta	340.5
0.01	Cu,W	283.1
0.05	Mo	172.9

Tab. 1: Breakdown voltage.

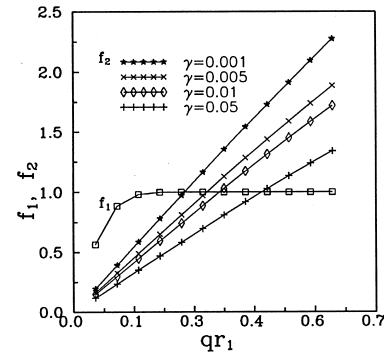


Fig. 1: Solution of transcendental equation.

Some results of the calculated breakdown voltage  $U_b$  are summarized in Tab. 1. The following input parameters were chosen ; Ar - gas,  $p = 4$  torr,  $V_i = 15, 7$  V,  $A = 14$  ionizations/cm-torr,  $B = 180$  V/cm-torr. The values of secondary emission coefficient  $10^{-4} < \gamma < 0.5$ , varied according to the material of spherical electrodes: Fe - 0.003, Ta - 0.008, W;Cu - 0.01, Hg - 0.1, Na - 0.3, and geometric factor:  $\delta = \frac{r_2-r_1}{r_1} = 10$ .

### 3. Numerical simulation

#### 3.1. The breakdown conditions

The simulation of the discharge between a thin wire and coaxial electrode or between sharp tip and sphere has been performed for argon gas at pressure  $p = (0.133 \div 26.6)$  kPa. The **breakdown potential**  $U_b$  and the **breakdown electric field**  $E_b$  has been determined for both polarity electrode. It is evident that the simulated dependencies (see Fig. 2 a - cylindrical , b -

spherical geometry) remind the **Paschen's curve** [2]. The discharge is more easily burned up for lower values of  $p \cdot \Delta R \leq 5.32 \text{ Pa}\cdot\text{m}$ , when the wire is anode. In spherical case, the ignition potential  $U_b$  is much higher than that for cylindrical one.

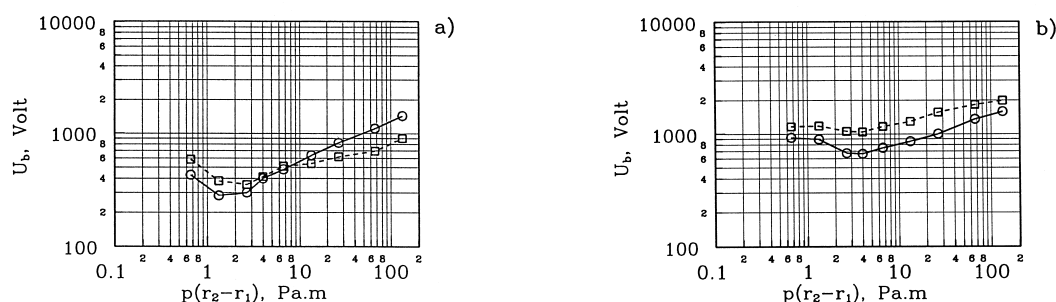


**Fig. 2:** The dependence of the breakdown potential  $U_b$  on  $p \cdot \Delta R$ , circle-wire (tip) is anode, box-wire (tip) is cathode.

### 3.2 Creation of double layer

The breakdown conditions for the discharge between thin wire and coaxial electrode (hydrogen,  $p = 13.3 \text{ kPa}$ ,  $r_1 = 0.5 \text{ mm}$ ,  $\Delta R = 5 \text{ mm}$ ) are determined from the time and space evolution of electron avalanche. Remarkable increase of the number of charged particles in the gap begins due to ionization process at  $t_{av} = 9.8 \times 10^{-10} \text{ s}$ , being followed by the electron (ion) ensemble rearrangement. The estimated value of breakdown potential was  $U_b = 785 \text{ V}$  and breakdown electric field was  $E_b = 4.5 \times 10^5 \text{ V/m}$ .

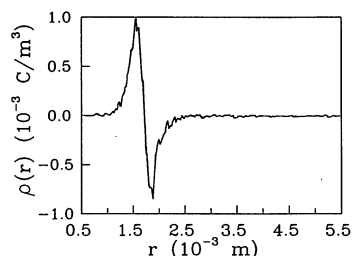


**Fig. 3:** The radial dependence of space charge of DL

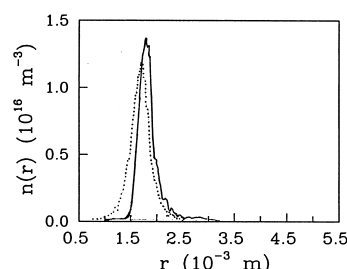


**Fig. 4:** The radial dependence of electron and ion density

The electrostatic **double layer** (DL) between the wire and cylinder is created with some time delay  $\Delta t = 1.9 \times 10^{-9} \text{ s}$ . The dimension of DL is  $\approx 1/5$  of the discharge gap and the center of DL (where the charge density  $\rho \approx 0$ ) lies at the radius  $r_* = 2.3 \cdot r_1$  (see Fig. 3). The positively charged part of DL lies near to the wire cathode while the negatively charged part is closer to the cylinder (see Fig. 4, electrons - full line, ions - dotted line). The total electric field is violated by the DL space charge.

The quasistationary state of electron and ion component in phase plane  $V_r - r$  illustrates the formation of DL (see Fig. 5 a,b). Around the cathode (wire) a thin layer exists in which the emitted electrons do not ionize the gas. The efficient ionization and excitation of atoms by emitted electrons occurs at distance  $r = 2 \cdot r_1$  next to the space where the stationary double layer is created. The rest part of discharge volume between the DL and cylinder anode is filled by electrons (points) and ions (circles) and serves as **reservoir of charged particles**. The quasineutrality condition holds in this major discharge part.

The size, location and charge density of DL depend on gas composition and pressure, electrode geometry and the value of applied voltage. For light elements the DL is narrower, lies near the cathode and the values of charge density are greater. For hydrogen at the pressure 13.3 kPa the maximum value of the inner potential is  $\psi_{max} \approx -62$  V and maximum value of inner electric field is  $\varepsilon_{max} \approx 2.4 \times 10^4$  V/m. The external electric field  $E$  has opposite direction and the ratio  $E/\varepsilon \approx 10$ .

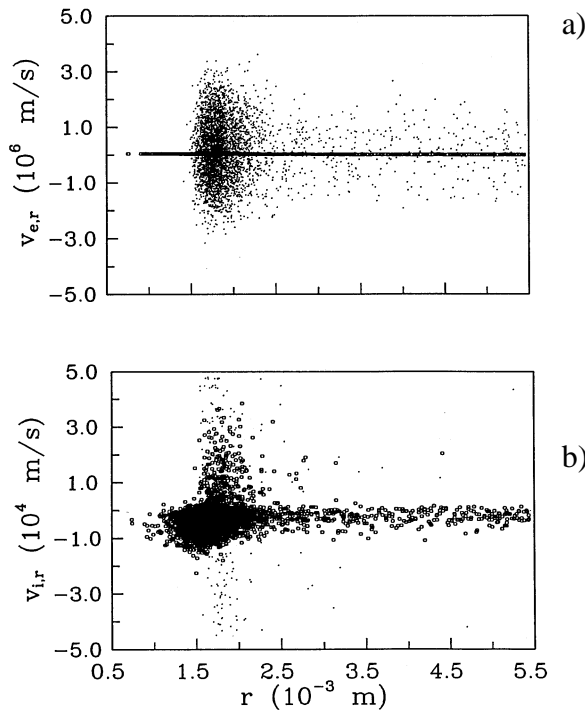


**Fig. 5:** The history of electron and ion velocities in  $V_r - r$  phase plain

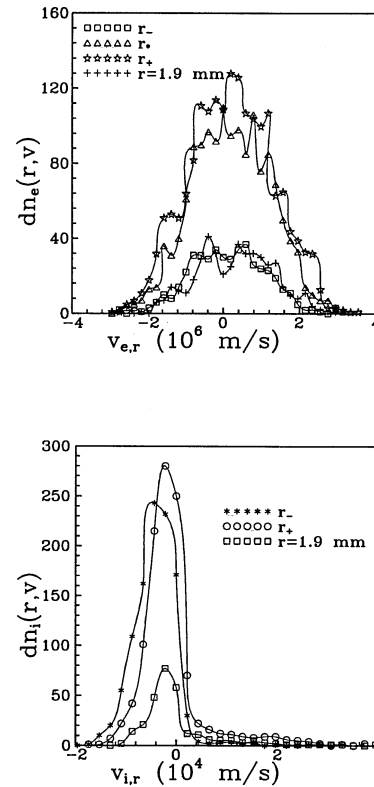


**Fig. 6:** The electron and ion distribution function

The electron and ion velocity distribution function were calculated (hydrogen,  $p = 13.3$  kPa,  $\Delta R = 5$  mm) at points  $r_-$  where  $\rho(r_-) = \rho_{max}$ ,  $r_*$  where  $\rho(r_*) \approx 0$ ,  $r_+$  where  $\rho(r_+) = \rho_{min}$  and at the point  $r = 1.9$  mm laying outside DL in the reservoir of charged particle. The maximum of **the electron distribution function** lies in positive part of velocity space (see Fig. 6a). Dominate electrons flowing to the anode (cylinder). The maximum of **the ion distribution function** lies in negative part of velocity space (see Fig. 6b). Dominate ions flowing to the cathode (wire), but the expressive **group of fast ions** propagates in opposite direction. The origin of this fast ion group is detected at the point  $r_+$ , where prevails the negative charge of the DL. The fast ion are accelerated here to the velocities  $10\times$  greater than the average velocity of ion component.

## References

- [1] E. Nasser.: Fundamentals of Gaseous Ionization & Plasma Electronics. Massachussets Institute of Technology Press, J. Wiley & Sons, Inc., 1971.
- [2] S.C. Brown.: Introduction to Electrical Discharges in Gases. Wiley, New York, 1966.
- [3] J. P. Verboncoeur, V. Vahedi, M. V.Alves, C. K.Birdsall.: Plasma Device 1 Dimensional Bounded Electrostatic Codes. Univ. of California, Berkeley, 1992.
- [4] Vrba P.: *XXIII ICPIG*, Toulouse, France, 17 - 22 July 1997, Proc. Contr. Papers Vol.II, p. 264-5.